a

a

1

a

a

a

1. Introduction

α

2. The meshfree methodology

$\square_p$

$$\square_I$$

$\square^{\psi}$

$\dot{\square}$

$\otimes$

$\square \cdot \square$

□ : □

$$div(\square)$$

$$grad(\square)$$

$grad^s(\square)$

2.1. Derivation of MPM procedure

$$\partial\Omega = \Gamma_d \bigcup \Gamma_n$$

$$\Gamma_d \cap \Gamma_n = \emptyset$$

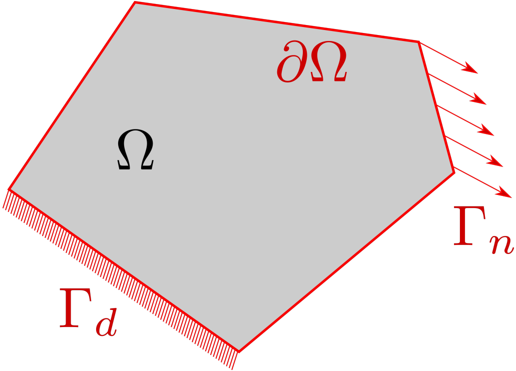

Figure 1: Description of the boundary-value-problem in a continuum. Red lines represents the closure $\partial\Omega$ of the domain Ω represented in gray.

$$\phi = (\varepsilon, \sigma)$$

$$\varepsilon = grad^s(\mathbf{u}), \tag{1}$$

$$\rho \frac{D\mathbf{v}}{Dt} = div(\sigma) + \rho\mathbf{b} \tag{2}$$

$$\mathfrak{R}^n$$

$\Re^n$

$$\sigma = \mathbf{D} \colon \varepsilon. \tag{3}$$

$$\frac{D\rho}{Dt} = \dot{\rho} + \rho div(\mathbf{v}) = 0. \tag{4}$$

$$\mathbf{u}^{\psi} \in \mathcal{H}_0^1(\Omega) = \{\mathbf{u}^{\psi} \in \mathcal{H}^1 \mid \mathbf{u}^{\psi} = \mathbf{0} \text{ on } \Gamma_d\}; \tag{5}$$

$$\int_{\Omega} \mathbf{u}^{\psi} \; d\Omega < \infty \quad \text{and} \quad \int_{\Omega} \varepsilon^{\psi} \; d\Omega < \infty. \tag{6}$$

$$\mathbf{u} \in \mathcal{H}_0^1$$

$$\mathbf{u}^{\psi} \in \mathcal{H}_0^1$$

$$\int_{\Omega} \rho \left(\frac{d\vec{v}}{dt} - \vec{b} \right) \cdot \vec{u}^{\psi} \, d\Omega = \int_{\Gamma_d} \vec{t} \cdot \vec{u}^{\psi} \, d\Gamma - \int_{\Omega} \sigma : \varepsilon^{\psi} \, d\Omega. \tag{7}$$

$$\Omega_p \subset \Omega$$

$$p = 1, 2 \ldots, N_p$$

N_p

$\vec{x}_p$

Ω_p

$$\vec{x}_p$$

$$\vec{v}_p$$

m_p

V_p

σ_p

$$\mathbf{u}_p^{\psi}$$

$$\int_{\Omega} \rho \; \frac{d\vec{v}}{dt} \cdot \mathbf{u}^{\psi} \; d\Omega = \frac{d\vec{v}_p}{dt} \cdot \mathbf{u}_p^{\psi} \; m_p. \tag{8}$$

$$\int_{\Omega} \sigma \ : \varepsilon^{\psi} \ d\Omega = \sigma_p \ : \varepsilon_p^{\psi} \ V_p. \tag{9}$$

$$\int_{\Omega} \rho \ \vec{b} \cdot \mathbf{u}^{\psi} \ d\Omega = \vec{b}_p \cdot \mathbf{u}_p^{\psi} \ m_p. \tag{10}$$

$$\int_{\Gamma_d} \vec{t}\, \mathbf{u}^{\psi}\ d\Gamma = \int_{\Gamma_d} \rho\ \vec{t^s} \cdot \mathbf{u}^{\psi}\ d\Gamma = \vec{t^s_p} \cdot \mathbf{u}^{\psi}_p\ h^{-1}\ m_p, \tag{11}$$

h

$$\vec{x}_I \ \ , I = 1, 2 \ldots, N_n$$

$$N_n$$

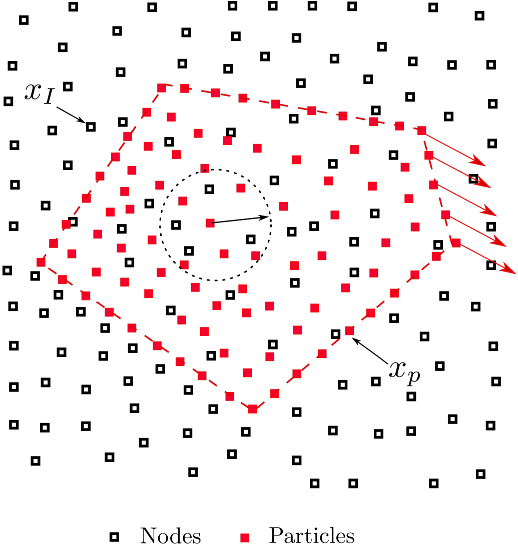

Figure 2: Description of the spatial discretization for domain presented in the figure ??. Blue mesh represent the background computational support, and the red mesh conforms the discretized continuum body.

p

$$\vec{u}_p = N_{Ip} \mathbf{u}_I$$

$$\vec{u}_p^{\psi} = N_{Ip} \mathbf{u}_I^{\psi}$$

$$\varepsilon_p = (\mathbf{u}_I \otimes grad(N_{Ip}))^s$$

$$\varepsilon_p^{\psi} = (\mathbf{u}_I^{\psi} \otimes grad(N_{Ip}))^s$$

$$\dot{\vec{p}}_I = \mathbf{m}_{IJ}\dot{\vec{v}}_J = \vec{f}_I^{int} + \vec{f}_I^{ext}, \tag{12}$$

$$\dot{\vec{p}}_I$$

I

$$\mathbf{m}_{IJ}$$

$$\mathbf{m}_{IJ} = N_{Ip} m_p N_{Jp}. \tag{13}$$

$\mathbf{m}_{IJ}^{lumped}$

$$\vec{f}_I^{int} = -\sigma_p \cdot grad(N_{Ip}) \frac{m_p}{\rho_p} \tag{14}$$

$$\vec{f}_I^{ext} = N_{Ip}\ \vec{b}_p\ m_p + N_{Ip}\ \vec{t}_p^{s}\ m_p h^{-1} \tag{15}$$

$$\sigma_p = \sigma_p(\varepsilon_p)$$

p

$$\dot{\varepsilon}_p$$

$$\dot{\varepsilon_p} = \frac{\Delta \varepsilon_p}{\Delta t} = \frac{1}{2} \left[grad(N_{Ip}) \;\; \otimes \vec{v}_I + \vec{v}_I \otimes grad(N_{Ip}) \;\right]. \tag{16}$$

$$\frac{D\rho}{Dt} = 0$$

$$\dot{\rho} = -\rho \; trace\left(\dot{\varepsilon}\right). \tag{17}$$

$k = 1 \ldots, Nt$

k

N_t

$$\dot{\vec{v}}_p = N_{Ip}\ \vec{a}_I, \quad and \quad \dot{\vec{x}}_p = N_{Ip}\ \vec{v}_I \tag{18}$$

2.2. MPM time integration scheme: the Explicit Predictor-Corrector proposal

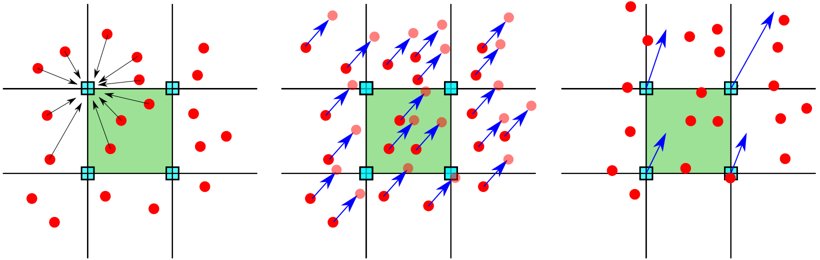

Figure 3: Description of the three steps in MPM standard algorithm.

$$\mathbf{v}_p^{k+1} = \mathbf{v}_p^k + \Delta t \; N_{Ip}^k \; \vec{a}_I^k \tag{19}$$

$$\mathbf{x}_p^{k+1} = \mathbf{x}_p^k + \Delta t \ N_{Ip}^k \ \vec{v}_I^k. \tag{20}$$

$$\mathbf{f}_I^{int,k}$$

m

$$\mathbf{x}_p^{k+1} = \mathbf{x}_p^k + \Delta t \ \frac{N_{Ip}^k \ \vec{p}_I^k}{\mathbf{m}_I}, \tag{21}$$

$$\mathbf{v}_p^{k+1} = \mathbf{v}_p^k + \Delta t \ \frac{N_{Ip}^k \ \vec{f}_I^k}{\mathbf{m}_I}. \tag{22}$$

α

$$\mathbf{v}_p^{k+1} = \mathbf{v}_p^k + \Delta t \; N_{Ip}^k \; \left[(1-\gamma) \; \mathbf{a}_I^k + \gamma \; \mathbf{a}_I^{k+1} \right], \tag{23}$$

$$\mathbf{x}_p^{k+1} = \mathbf{x}_p^k + N_{Ip}^k \left[\Delta t \ \vec{v}_I^k + \Delta t^2 \left((\frac{1}{2} - \beta) \ \vec{a}_I^k + \beta \ \vec{a}_I^{k+1} \right) \right], \qquad (24)$$

$$\mathbf{a}_p^{k+1} = N_{Ip}^k \ \vec{a}_I^{k+1}. \tag{25}$$

$\gamma = 0.5$

$$\beta = 0$$

$$\mathbf{M}_{IJ}\ddot{\mathbf{d}}_J + \mathbf{C}_{IJ}\dot{\mathbf{d}}_J + \mathbf{K}_{IJ}\mathbf{d}_J = \mathbf{F}_I.$$

$$(k+1)$$

$$\vec{\tilde{v}}_I^{k+1}$$

$$\vec{\tilde{v}}_I^{k+1} = \vec{v}_I^k + (1 - \gamma)\ \Delta t\ \vec{a}_I^k. \tag{26}$$

$\gamma \geq 0$

$$O(\Delta t^3)$$

$\gamma = 0.5$

$$0 < \gamma \leq 0.25$$

Φ_p

Φ_I

$$\Phi_I = \frac{m_p N_{Ip} \Phi_p}{m_I}. \tag{27}$$

$$\tilde{\vec{v}}_I^{k+1} = \underbrace{\frac{N_{Ip}^k m_p \vec{v}_p^k}{m_I}}_{\vec{v}_I^k} + (1-\gamma)\ \Delta t\ \underbrace{\frac{N_{Ip}^k m_p \vec{a}_p^k}{m_I}}_{\vec{a}_I^k} . \tag{28}$$

$$\tilde{\vec{v}}_I^{k+1} = \frac{N_{Ip}^k m_p (\vec{v}_p^k + (1-\gamma)\ \Delta t\ \vec{a}_p^k)}{m_I}. \tag{29}$$

$$\vec{v}_I^{k+1} = \vec{v}_I^{pred} + \gamma \; \Delta t \; \frac{\vec{f}_I^{k+1}}{\mathbf{m}_I^{k+1}}. \tag{30}$$

$$\vec{a}_p^{k+1} = \frac{N_{Ip}^k \vec{f}_I^k}{\mathbf{m}_I^k} \tag{31}$$

$$\vec{v}_p^{k+1} = \vec{v}_p^n + \Delta t \ \frac{N_{Ip}^k \ \vec{f}_I^k}{\mathbf{m}_I^k} \tag{32}$$

$$\vec{x}_p^{k+1} = \vec{x}_p^n + \Delta t \ N_{Ip}^k \ \vec{v}_I^k + \frac{1}{2}\Delta t^2 \ \frac{N_{Ip}^k \ \vec{f}_I^k}{\mathbf{m}_I^k}. \tag{33}$$

1: **Update mass matrix**:

$$\mathbf{m}_I = N_{Ip}^k \; m_p,$$

2: **Explicit Newmark Predictor**:

$$\vec{v}_I^{pred} = \frac{N_{Ip}^k m_p (\vec{v}_p^k + (1-\gamma)\;\Delta t\;\vec{a}_p^k)}{m_I}$$

3: **Impose essential boundary conditions**:
At the fixed boundary, set $\vec{v}_I^{pred} = 0$.
4: **Deformation tensor increment calculation**.

$$\dot{\varepsilon}_p^{\;k+1} = \left[\vec{v}_I^{pred} \otimes grad(N_{Ip}^{k+1})\right]^s$$
$$\Delta\varepsilon_p^{k+1} = \Delta t\;\dot{\varepsilon}_p^{\;k+1}$$

5: **Update the density field**:

$$\rho_p^{k+1} = \frac{\rho_p^k}{1 + trace\left[\Delta\varepsilon_p^{k+1}\right]}.$$

6: **Balance of forces calculation**:
Calculate the total grid nodal force $\vec{f}_I^{k+1} = \vec{f}_I^{int,k+1} + \vec{f}_I^{ext,k+1}$ by evaluating (**??**) and (**??**) in the time step $k+1$. In those nodes where $\frac{\partial \mathbf{v}_I^k}{\partial t}\Big|_{\Gamma_d} = 0$, the acceleration is fixed to zero and nodal forces are stored as reactions.
7: **Explicit Newmark Corrector**:

$$\vec{v}_I^{k+1} = \vec{v}_I^{pred} + \gamma\;\Delta t\;\frac{\vec{f}_I^{k+1}}{\mathbf{m}_I^{k+1}}$$

8: **Update particles lagrangian quantities**:

$$\vec{a}_p^{k+1} = \frac{N_{Ip}^k \vec{f}_I^k}{\mathbf{m}_I^k}$$
$$\vec{v}_p^{k+1} = \vec{v}_p^n + \Delta t\;\frac{N_{Ip}^k\;\vec{f}_I^k}{\mathbf{m}_I^k}$$
$$\vec{x}_p^{k+1} = \vec{x}_p^n + \Delta t\;N_{Ip}^k\;\vec{v}_I^k + \frac{1}{2}\Delta t^2\;\frac{N_{Ip}^k\;\vec{f}_I^k}{\mathbf{m}_I^k}$$

9: **Reset nodal values**

2.3. Local Max-Ent approximants

β

β

$$N_I(\vec{x})$$

$$H(p_1(\vec{x}), \ldots, p_n(\vec{x})) = -\sum_{I=1}^{N_n} p_I(\vec{x}) \log p_I \tag{34}$$

$p_I(\vec{x})$

$$N_I(\vec{x})$$

$$
\text{(LME) Maximize } H(N_I) \equiv -\sum_{I}^{N_n} N_I(\vec{x}) \log N_I
$$

$$
\text{subject to } \begin{cases} N_I \geq 0, \ \text{I=1, ..., n} \\ \\ \sum_{I=1}^{N_n} N_I = 1 \\ \sum_{I=1}^{N_n} N_I \vec{x}_I = \vec{x} \end{cases}
$$

$$\text{(RAJ) For fixed } \vec{x} \text{ minimize } U(\vec{x}_p, N_I) \equiv \sum_I N_I |\vec{x}_p - \vec{x}_I|^2$$

$$\text{subject to } \begin{cases} N_I \geq 0, \ \text{I=1, ..., n} \\ \sum_{I=1}^{N_n} N_I = 1 \\ \sum_{I=1}^{N_n} N_I \vec{x}_I = \vec{x} \end{cases}$$

$$
(\mathrm{LME})_\beta \text{ For fixed } \vec{x} \text{ minimize } f_\beta(\vec{x}, N_I) \equiv \beta U(\vec{x}, N_I) - H(N_I)
$$

$$
\text{subject to } \begin{cases} N_I \geq 0, \text{ I=1, ..., n} \\ \\ \sum_{I=1}^{N_n} N_I = 1 \\ \\ \sum_{I=1}^{N_n} N_I \vec{x}_I = \vec{x} \end{cases}
$$

β

$\beta \in (0, \infty)$

β

$$N_I^*(\vec{x}) = \frac{\exp\left[-\beta\ |\vec{x} - \vec{x}_I|^2 + \vec{\lambda}^* \cdot (\vec{x} - \vec{x}_I)\right]}{Z(\vec{x}, \vec{\lambda}^*)} \tag{35}$$

$$Z(\vec{x},\vec{\lambda}) = \sum_{I=1}^{N_n} \exp\left[-\beta\,\left|\vec{x}-\vec{x}_I\right|^2 + \vec{\lambda}\cdot\left(\vec{x}-\vec{x}_I\right)\right] \tag{36}$$

$$\vec{\lambda}^*(\vec{x})$$

$$\log Z(\vec{x}, \vec{\lambda})$$

$$\partial \vec{\lambda}$$

J

$$\mathbf{J}(\vec{x}, \vec{\lambda}, \beta) \equiv \frac{\partial \vec{r}}{\partial \vec{\lambda}} \tag{37}$$

$$\vec{r}(\vec{x}, \vec{\lambda}, \beta) \equiv \frac{\partial \log Z(\vec{x}, \vec{\lambda})}{\partial \vec{\lambda}} = \sum_{I}^{N_n} p_I(\vec{x}, \vec{\lambda}, \beta)\,(\vec{x} - \vec{x}_I) \tag{38}$$

$$\nabla N_I^*$$

$$\nabla N_I^* = N_I^* \left(\nabla f_I^* - \sum_J^{N_n} N_J^* \nabla f_J^* \right) \tag{39}$$

$$f_I^*(\vec{x}, \vec{\lambda}, \beta) = -\beta \, |\vec{x} - \vec{x}_I|^2 + \vec{\lambda} \, (\vec{x} - \vec{x}_I) \tag{40}$$

β

$$\nabla N_I^* = -N_I^* \left(\mathbf{J}^*\right)^{-1} \left(\vec{x} - \vec{x}_I\right) \tag{41}$$

β

$$\gamma = \beta h^2$$

h

N_I

$$\exp(-\beta\vec{r})$$

-6

$d + 1$

d

$$d + 1$$

d

γ

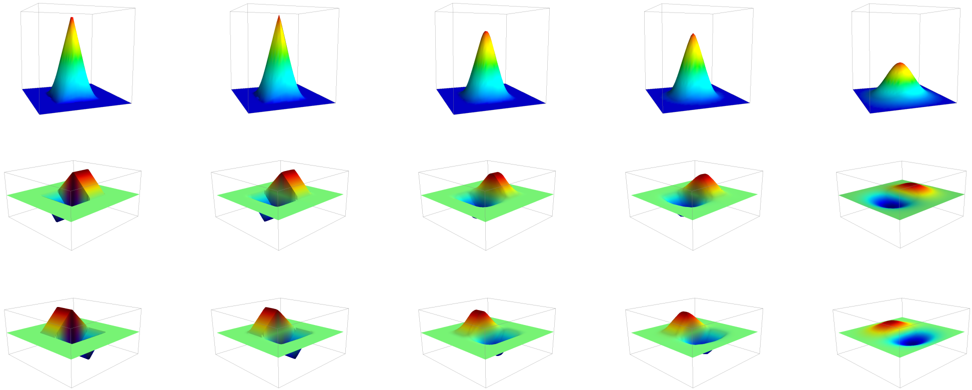

(a) Q4 (b) LME_{17} (c) uGIMP (d) LME_{10} (e) LME_5

Figure 4: Comparative of linear piecewise shape functions (Q4) and uGIMP shape functions *versus* LME approximation for a two-dimensional arrangement of nodes, and spatial derivatives for several values of $\gamma = \beta/h^2$.

3. Application to linear elasticity dynamic problems.

3.1. Dyka's bar [?]

$$\mathbf{v}\big|_{x=L} = 0$$

$$\sigma\big|_{x=0} = 0$$

$$\mathbf{v}_o = -5\ m/s$$

$7833\ kg/m3$

0

$$200 \cdot 10^9 \ Pa$$

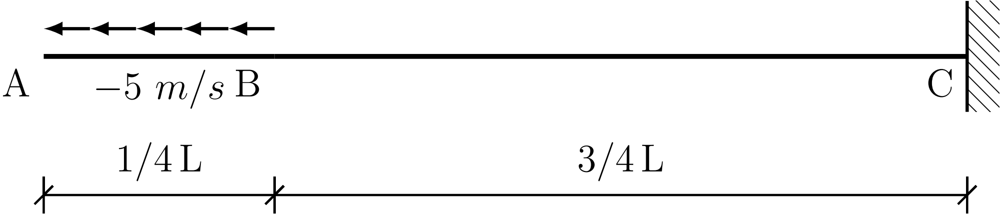

Figure 5: Geometrical description of the Dyka [**?**] bar.

$$Cel = \max\{\max_{p\in\Omega_p}\{\mathbf{v}_p\}, \max_{p\in\Omega_p}\{\sqrt{\frac{E_p}{\rho_p}}\}\}. \tag{42}$$

$$RMS = \sqrt{\frac{1}{N}\sum_{p}^{N}\left(\mathbf{v}_p - \hat{\mathbf{v}}_p\right)^2}, \tag{43}$$

$\mathbf{V}p$

$\hat{\mathbf{V}}_p$

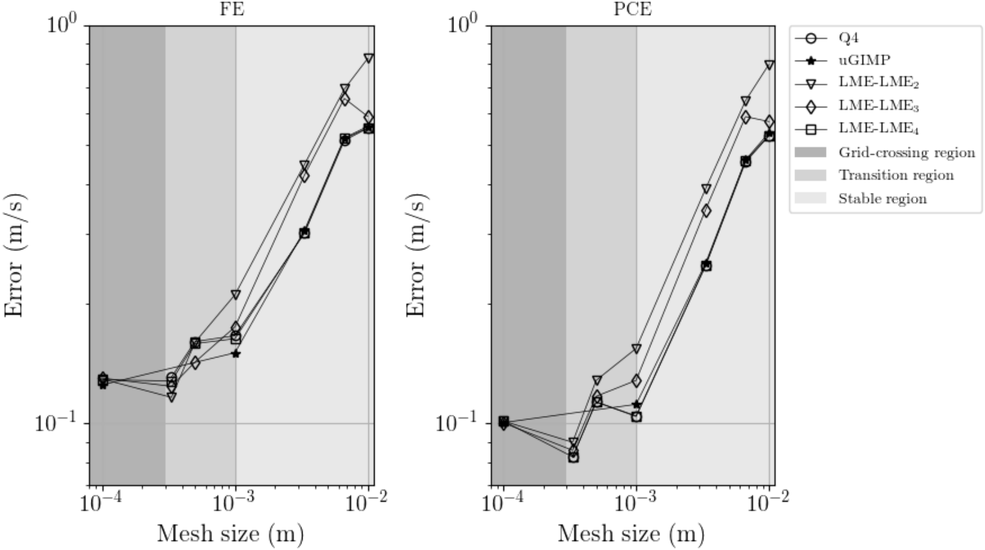

Figure 6: Velocity error evolution at the point A in the Dyka's bar , convergence plots for FE and NPC. The plot is subdivided with colours, the darker part of the diagram shows coincides when the relative movement of the particles is large enough to produce the grid crossing phenomena. The lightest part of the diagram coincides when the relative movement of the particles in negligible in comparison with the mesh size. And in the middle region a transition behaviour take place.

$$6E^5$$

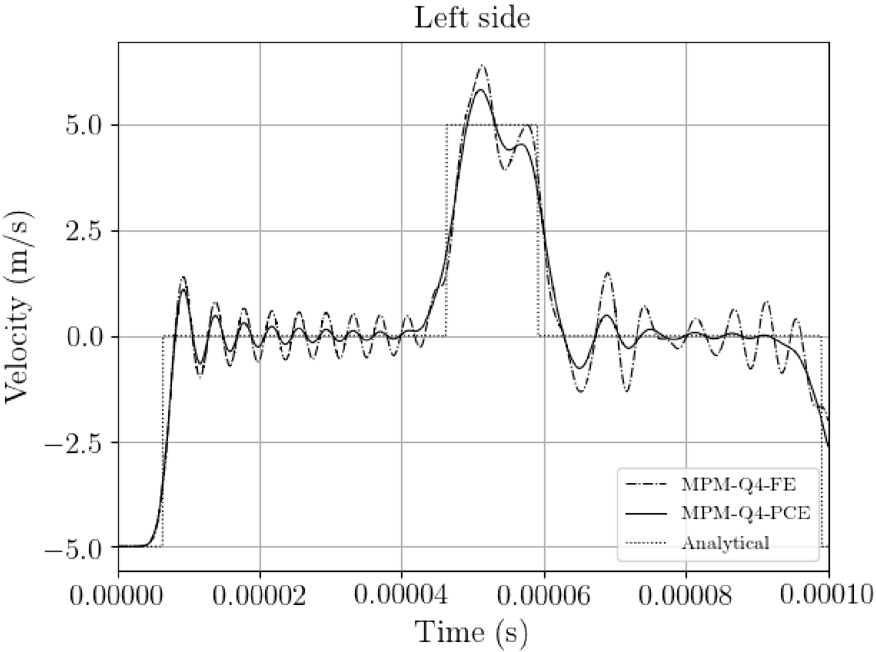

Figure 7: Comparative of the NPC *versus* the FE. In the picture the velocity evolution at the point in the bar left side is plotted.

γ

β

β

γ

γ

γ

γ

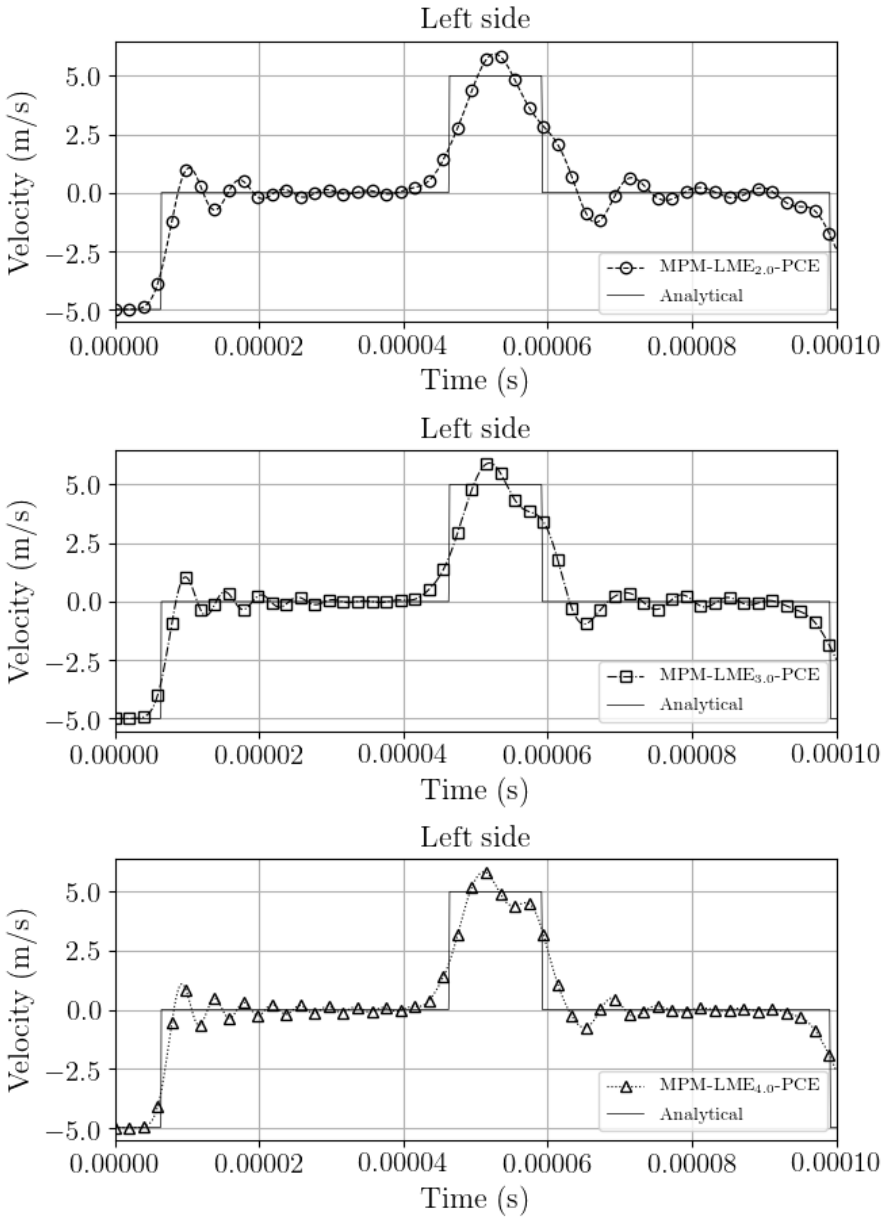

Figure 8: Sensitive of LME approximants performance to changes in the dimensionless regularization parameter $\gamma = \beta/h^2$. To illustrate it, the velocity evolution at the point in the bar left side is plotted.

γ

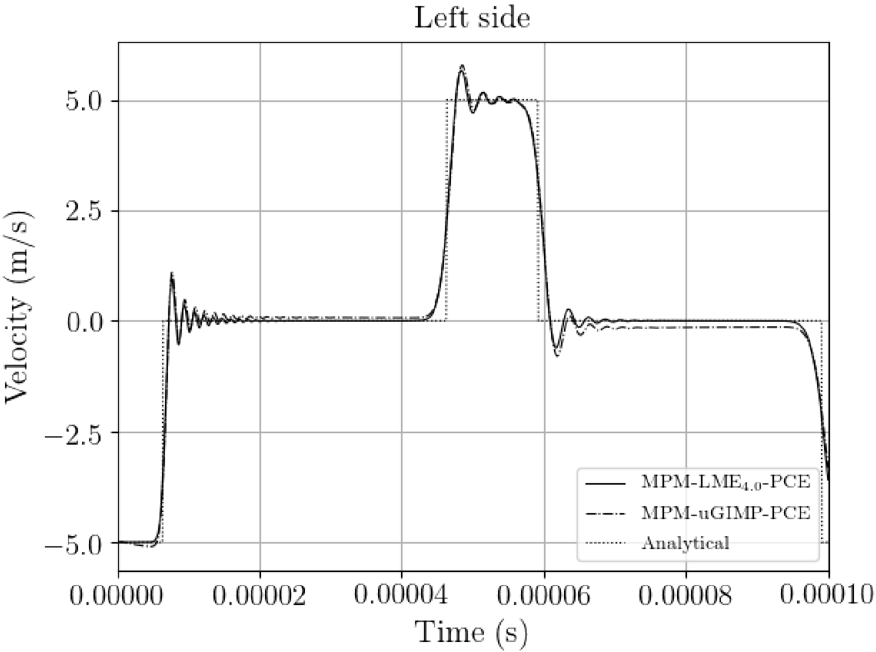

Figure 9: Velocity evolution at the point in the bar left side.

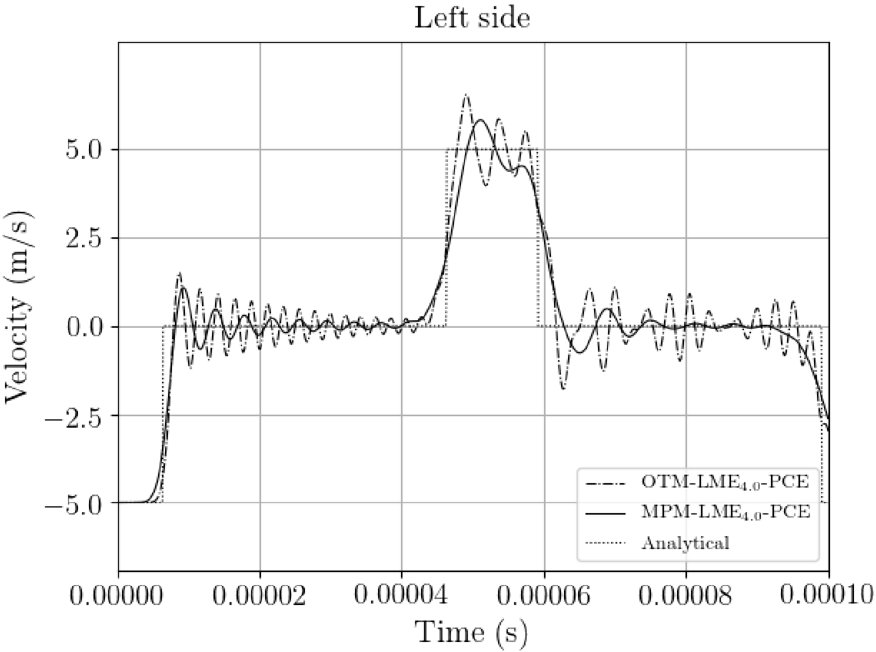

Figure 10: Velocity evolution at the point in the bar left side.

3.2. Rigid block

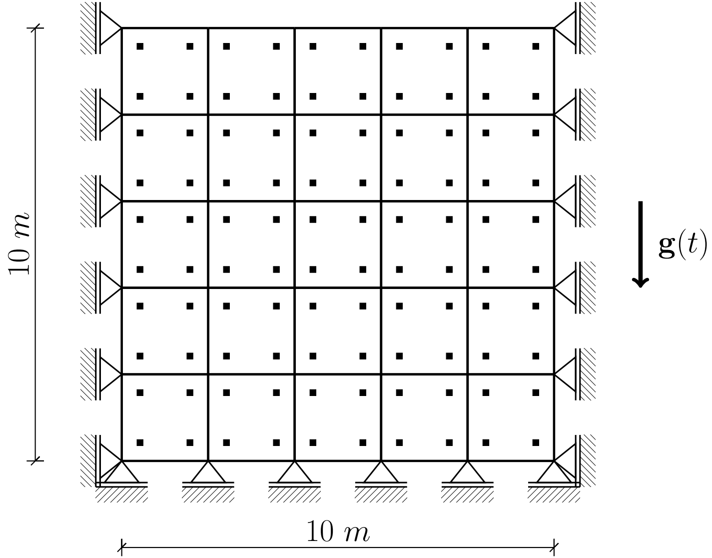

Figure 11: Geometrical description of a soil block

.

$$6 \cdot 10^3 \ kg/m^3$$

0

$5 \ MPa$

m/s

$$\mathbf{g}(t) = \begin{cases} 0.5\mathbf{g}(\sin(\frac{2t\pi}{T} - \frac{\pi}{2}) + 1) & \text{if } t \leq T/2 \\ \mathbf{g} & \text{if } t > T/2 \end{cases} \tag{44}$$

$$\Delta x = 2\ m$$

$5.2 MPa$

$$\sigma_{yy} = \rho g h_y$$

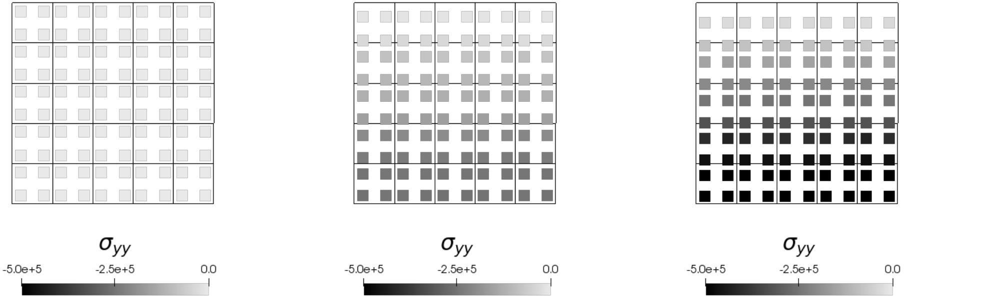

(a) t = 0 seconds. (b) t = 5 seconds. (c) t = 20 seconds

Figure 12: Vertical normal stress and position of material points during the loading process for a soft soil ($E = 5\ MPa$, $\rho_0 = 6 \cdot 10^3\ kg/m^3$). Numerical parameters considered for the simulation are : Local *max-ent* shape function $\gamma = 3$ and explicit PC scheme with CFL 0.1.

$$\gamma = 0.8$$

$$\gamma = 3.0$$

γ

γ

$$\beta(\mathbf{x})$$

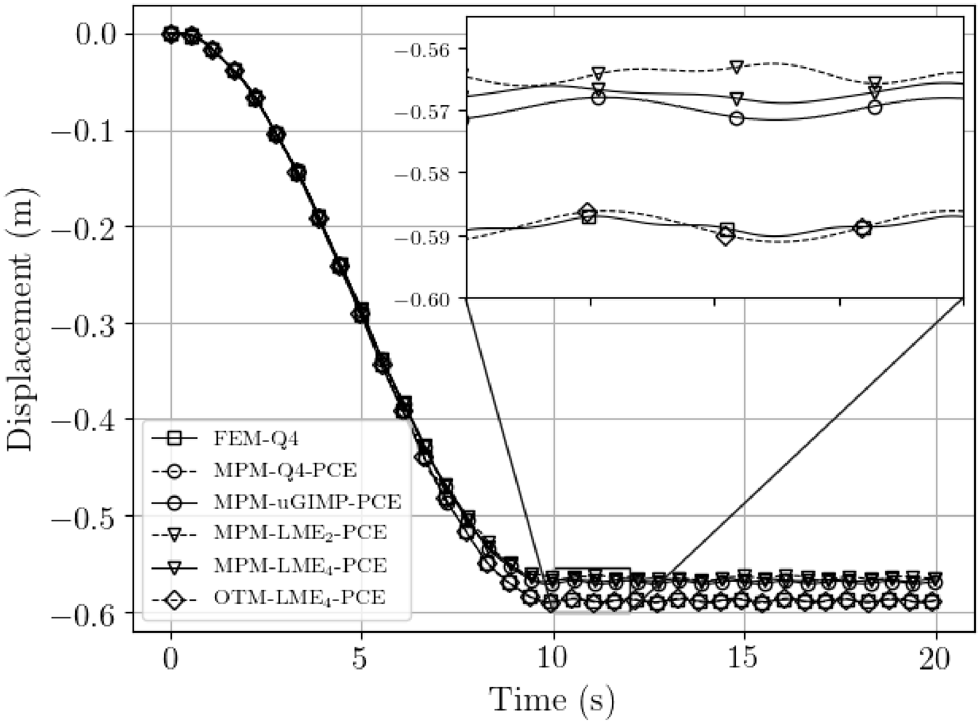

Figure 13: Comparative of the vertical displacement evolution in a point located in the free surface employing different interpolation schemes and numerical techniques.

4. Conclusions

$$u - p_w$$

$$\beta(\mathbf{x})$$

β

Conflict of interest

Acknowledgements

Appendix A. The analytical solution of the 1D Dyka benchmark

$$\rho \ \frac{\partial v}{\partial t} = \frac{\partial \sigma}{\partial x}, \tag{A.1}$$

$$\frac{\partial \sigma}{\partial t} = E \frac{\partial \varepsilon}{\partial t}, \tag{A.2}$$

E

$$\frac{\partial \varepsilon}{\partial t} = \frac{\partial v}{\partial x}. \tag{A.3}$$

$$\frac{\partial v}{\partial t} = \frac{1}{\rho} \ \frac{\partial \sigma}{\partial x}, \tag{A.4}$$

$$\frac{\partial \sigma}{\partial t} = E \ \frac{\partial v}{\partial x}. \tag{A.5}$$

$$\frac{\partial^2 u}{\partial t^2} = \frac{E}{\rho} \frac{\partial^2 u}{\partial x^2} = c^2 \frac{\partial^2 u}{\partial x^2} \tag{A.6}$$

$$c = \sqrt{\frac{E}{\rho}}$$

$$\frac{\partial}{\partial t}\begin{bmatrix}\sigma\\ v\end{bmatrix}+\begin{bmatrix}0 & -E\\ -1/\rho & 0\end{bmatrix}\begin{bmatrix}\frac{\partial\sigma}{\partial x}\\ \frac{\partial v}{\partial x}\end{bmatrix}=\mathbf{0}. \tag{A.7}$$

$$\frac{\partial \phi}{\partial t} + \mathbf{A}\frac{\partial \phi}{\partial x} = \mathbf{0}. \tag{A.8}$$

ϕ

A

$$\phi = \begin{bmatrix} \sigma \\ v \end{bmatrix}, \quad \mathbf{A} = \begin{bmatrix} 0 & -E \\ -1/\rho & 0 \end{bmatrix}.$$

A

$$\lambda = \pm\sqrt{\frac{E}{\rho}}$$

A

n

$$\{\lambda_1, \ldots, \lambda_i, \ldots \lambda_n\}$$

n

$$\{\vec{x}^1, \ldots, \vec{x}^i, \ldots \vec{x}^n\}$$

$$\mathbf{A}\vec{x} = \lambda\vec{x}$$

P

n

X

$$\mathbf{P} = \{\vec{x}^1, \vec{x}^2, \vec{x}^3, \ldots \vec{x}^n\}. \tag{A.9}$$

A

P

$$\Lambda = \mathbf{P}^{-1}\mathbf{A}\ \mathbf{P}, \tag{A.10}$$

$$\Lambda_{ii} = \lambda_i$$

R

$$\phi = \mathbf{P} \ \Re. \tag{A.11}$$

P

$$d\vec{\Re} = \frac{\partial \Re}{\partial t} dt + \frac{\partial \Re}{\partial x} dx = \mathbf{P}^{-1} \left(\frac{\partial \phi}{\partial t} dt + \frac{\partial \phi}{\partial x} dx \right) \tag{A.12}$$

$$\frac{\partial \mathfrak{R}}{\partial t} = \mathbf{P}^{-1}\frac{\partial \phi}{\partial t}, \qquad \frac{\partial \mathfrak{R}}{\partial x} = \mathbf{P}^{-1}\frac{\partial \phi}{\partial x} \tag{A.13}$$

$$\mathbf{P}^{-1}$$

$$\mathbf{P}^{-1}\frac{\partial \phi}{\partial t} + \left(\mathbf{P}^{-1}\mathbf{A}\mathbf{P}\right)\mathbf{P}^{-1}\frac{\partial \phi}{\partial x} = \mathbf{0} \tag{A.14}$$

$$\frac{\partial \Re}{\partial t} + \Lambda \frac{\partial \Re}{\partial x} = \mathbf{0} \tag{A.15}$$

n

Λ

$$\Re^{(i)} = F^{(i)}\left(x - \lambda^{(i)}t\right) \tag{A.16}$$

n

$$\mathfrak{R}_i$$

$$\Re_i(x, t = 0) = h_i(x)$$

P

$$\mathbf{P} = \begin{bmatrix} -\sqrt{E\rho} & \sqrt{E\rho} \\ 1 & 1 \end{bmatrix}$$

$$\mathbf{P}^{-1}$$

$$\Re^{I} = \frac{1}{2\sqrt{\rho E}} \left(-\sigma + v \ \sqrt{\rho E} \right) \tag{A.17}$$

$$\Re^{II} = \frac{1}{2\sqrt{\rho E}} \left(\sigma + v \ \sqrt{\rho E} \right) \tag{A.18}$$

$$v = \Re^{I} + \Re^{II} \quad , \quad \sigma = \sqrt{E\rho}\left(\Re^{II} - \Re^{I}\right) \tag{A.19}$$

$$\Re^{II} = 0 \quad and \quad v_{x=L} = 0 \quad \Rightarrow \quad \sigma_{x=L} = -2\sqrt{\rho E}\ \Re^{I}$$

$$\Re^{I} = 0 \quad and \quad \sigma_{x=0} = 0 \quad \Rightarrow \quad v_{x=0} = 2\Re^{II}$$